Inorg. Chem. **2004**, *43*, 6568–6578

Synthesis, Characterization, and Structures of Copper(II)–Thiosulfate Complexes Incorporating Tripodal Tetraamine Ligands

Adam J. Fischmann, Andrew C. Warden, Jay Black, and Leone Spiccia*

School of Chemistry, Monash University, Victoria 3800, Australia

Received June 2, 2004

The reaction of $[Cu(L)(H_2O)]^{2+}$ with an excess of thiosulfate in aqueous solution produces a blue to green color change indicative of thiosulfate coordination to Cu(II) [L = tren, Bz_3tren, Me_6tren, and Me_3tren; tren = tris(2-aminoethyl)amine, Bz_3tren = tris(2-benzylaminoethyl)amine, Me_6tren = tris(2,2-dimethylaminoethyl)amine, and Me_3tren = tris(2-methylaminoethyl)amine]. In excess thiosulfate, only $[Cu(Me_6tren)(H_2O)]^{2+}$ promotes the oxidation of thiosulfate to polythionates. Products suitable for single-crystal X-ray diffraction analyses were obtained for three thiosulfate complexes, namely, $[Cu(tren)(S_2O_3)]\cdot H_2O$, $[Cu(Bz_3tren)(S_2O_3)]\cdot MeOH$, and $(H_3Me_3tren)[Cu(Me_3tren)(S_2O_3)]_2(ClO_4)_3$. Isolation of $[Cu(Me_6tren)(S_2O_3)]$ was prevented by its reactivity. In each complex, the copper(II) center is found in a trigonal bipyramidal (TBP) geometry consisting of four amine nitrogen atoms, with the bridgehead nitrogen in an axial position and an S-bound thiosulfate in the other axial site. Each structure exhibits H bonding (involving the amine ligand, thiosulfate, and solvent molecule, if present), forming either 2D sheets or 1D chains. The structure of $[Cu(Me_3tren)(MeCN)](ClO_4)_2$ was also determined for comparison since no structures of mononuclear Cu(II)–Me_3tren complexes have been reported. The thiosulfate binding constant was determined spectrophotometrically for each Cu(II)–amine complex. Three complexes yielded the highest values reported to date [$K_f = (1.82 \pm 0.09) \times 10^3$ M^{-1} for tren, $(4.30 \pm 0.21) \times 10^4$ M^{-1} for Bz_3tren, and $(2.13 \pm 0.05) \times 10^3$ M^{-1} for Me_3tren], while for Me_6tren, the binding constant was much smaller (40 ± 10 M^{-1}).

Introduction

The hydrometallurgical processing of gold requires an oxidant to convert metallic gold to either Au(I) or Au(III) ions and a ligand to complex the oxidized gold and stabilize it in aqueous solution. In the traditional cyanidation process, oxygen is used as the oxidant and cyanide as the complexing agent.[1] Growing concerns about the potential environmental hazards presented by the production, transport, and use of cyanide are stimulating interest in alternative gold-processing methods.[2−4] One promising, more benign alternative utilizes a copper(II) tetraamine catalyst $\{[Cu(NH_3)_4]^{2+}\}$ to oxidize native gold to Au(I) and thiosulfate ($S_2O_3^{2-}$) as the complexing ligand, forming $[Au(S_2O_3)_2]^{3-}$.[3]

$$Au^0(s) + 2S_2O_3^{2-} \leftrightarrows [Au(S_2O_3)_2]^{3-} + e^- \quad (1)$$

$$[Cu(NH_3)_4]^{2+} + 3S_2O_3^{2-} + e^- \leftrightarrows [Cu(S_2O_3)_3]^{5-} + 4NH_3 \quad (2)$$

The Cu(II) complex oxidizes gold at a much faster rate than oxygen, increasing the efficiency of the process.[3] In the reaction, the $[Cu(NH_3)_4]^{2+}$ catalyst is converted into the Cu(I) species, and for the process to continue, the catalyst needs to be regenerated, usually by air oxidation. An impediment to the industrial use of the thiosulfate leaching process is that $[Cu(NH_3)_4]^{2+}$ also oxidizes thiosulfate, initially to tetrathionate ($S_4O_6^{2-}$) (eq 3).[3] This leads to unacceptable consumption of thiosulfate and has an adverse impact on economic viability.

$$2[Cu(NH_3)_4]^{2+} + 8S_2O_3^{2-} \leftrightarrows 2[Cu(S_2O_3)_3]^{5-} + S_4O_6^{2-} + 8NH_3 \quad (3)$$

We have embarked on a search for alternative Cu(II) complexes that effectively and rapidly oxidize gold but do

* Author to whom correspondence should be addressed. E-mail: leone.spiccia@sci.monash.edu.au. Fax: +61-3-9905-4597.

(1) Sparrow, G. J.; Woodcock, J. T. *Miner. Process. Extr. Metall. Rev.* **1995**, *14*, 193−247.
(2) Grosse, A. C.; Dicinoski, G. W.; Shaw, M. J.; Haddad, P. R. *Hydrometallurgy* **2003**, *69*, 1−21.
(3) Aylmore, M. G.; Muir, D. M. *Miner. Eng.* **2001**, *14*, 135−174.
(4) Molleman, E.; Dreisinger, D. *Hydrometallurgy* **2002**, *66*, 1−21.

10.1021/ic0492800 CCC: $27.50
Published on Web 09/14/2004

not oxidize thiosulfate.[5] A feature to emerge from these studies is that color changes, presumably signifying Cu(II)−thiosulfate complexation, occur immediately on the addition of thiosulfate to many Cu(II) complexes. As indicated in our previous publication, subsequent reactions, leading to thiosulfate oxidation, are sufficiently fast to prevent isolation and allow full analysis of the product.[5]

In fact, few constants (K_f) for the coordination of thiosulfate to Cu(II) are available,[6−9] and at the present time, only one crystal structure of a Cu(II)−thiosulfate complex has been reported in which thiosulfate occupies the axial position in a square pyramidal geometry.[10] In the course of our studies, the Cu(II) complexes of tren [tris(2-aminoethyl)amine], Bz_3tren [tris(2-benzylaminoethyl)amine], Me_3tren [tris(2-methylaminoethyl)amine], and Me_6tren [tris(2,2-dimethylaminoethyl)amine] were found to react with thiosulfate in aqueous solution to form complexes which, with the exception of Me_6tren, are stable for long periods under certain conditions. This has enabled the thiosulfate binding constant to be measured in aqueous solution and the isolation, characterization, and X-ray structure analysis of $[Cu(tren)(S_2O_3)]\cdot H_2O$, $[Cu(Bz_3tren)(S_2O_3)]\cdot MeOH$, and $(H_3Me_3tren)[Cu(Me_3tren)(S_2O_3)]_2(ClO_4)_3$ reported herein. Our study was aided by the ability of the tetradentate ligands to bind strongly to four of five coordination sites on a TBP Cu(II) center[11] [tren,[12] $\log K = 19.58$; Me_3tren,[13] $\log K = 19.11$; Me_6tren,[12] $\log K = 15.65$; and Bz_3tren, $\log K = 15.10$ (vide infra)], leaving only one site available for the coordination of other ligands.

Results and Discussion

Exploratory Studies. The addition of thiosulfate to solutions of $[Cu(L)(H_2O)]^{2+}$ was found to cause a blue to green color change reflecting coordination of thiosulfate (eq 4), which results in a thiosulfate-S to Cu(II) ligand-to-metal charge transfer (LMCT) transition between 300 and 450 nm (Figure 1).

$$[Cu(L)(H_2O)]^{2+} + S_2O_3^{2-} \leftrightarrows [Cu(L)(S_2O_3)] + H_2O \quad (4)$$

The intensity of the LMCT bands varies with the thiosulfate concentration, but there was no change in the spectrum over many days when excess thiosulfate was present (the Me_6tren complex was the only exception). In the case of tren, when the total concentration of Cu(II) was in excess over thiosulfate, the thiosulfate complex underwent a decomposition reaction which involved several processes.[5] For the conditions of $[Cu]_{total} = 2.5$ mM and $[S_2O_3^{2-}] = 0.25$ mM, the rate constant of the final (slowest) process was $(1.7 \pm 0.1) \times 10^{-4}$ s^{-1}, and at the end of the reaction, the spectrum matched that of $[Cu(tren)(H_2O)]^{2+}$. The Cu(I) species that formed did not absorb between 300 and 500 nm, the wavelength range monitored.[5] The formation constant for $[Cu(Me_6tren)(S_2O_3)]$ is the smallest in the series (vide infra). Moreover, for this system, bleaching of the solution that is indicative of thiosulfate oxidation was observed for all thiosulfate/Cu(II) ratios examined.

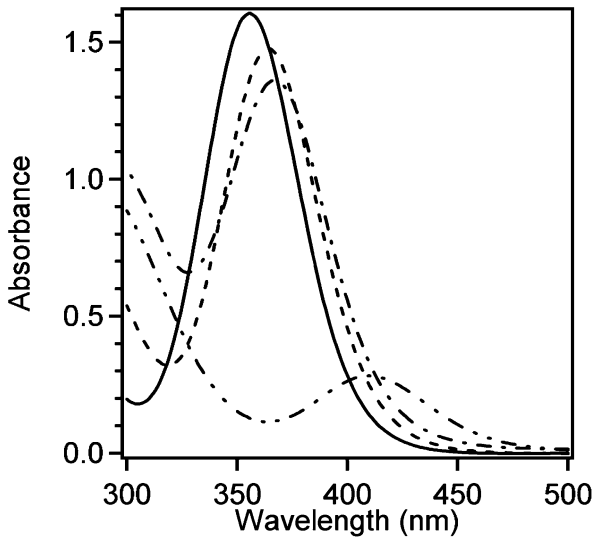

Figure 1. UV−visible spectra of aqueous solutions of $[Cu(L)(H_2O)]^{2+}$ and $S_2O_3^{2-}$, L = tren (—), Me_3tren (— —), Bz_3tren* (— · —), and Me_6tren (— ·· —). $[Cu]_{total} = 0.25$ mM; $[S_2O_3^{2-}] = 25$ mM. For Bz_3tren*, $[Cu]_{total} = 0.5$ mM, $[S_2O_3^{2-}] = 2.5$ mM, and absorbance is scaled by a factor of one-half.

Synthesis and Characterization. Crystals of $[Cu(tren)(S_2O_3)]\cdot H_2O$ were deposited on slow evaporation of a concentrated aqueous solution of $[Cu(tren)(H_2O)](ClO_4)_2$ and $Na_2S_2O_3\cdot 5H_2O$ (1:1 molar ratio). Figure 2 shows that the four absorption maxima found in the UV−visible diffuse reflectance spectrum of the solid match those in the spectrum of an aqueous solution of $[Cu(tren)(H_2O)]^{2+}$ and $S_2O_3^{2-}$, confirming that the solution and solid-state chromophores must be structurally similar.

The IR spectrum exhibits absorptions indicating the presence of water, tren, and thiosulfate and the absence of perchlorate. The position of the asymmetric stretch of the SO_3 group, $\nu_{as}(SO_3)$, normally found in the 1100−1200 cm^{-1} region, is diagnostic of the thiosulfate binding mode;[14] S-bridging (>1175 cm^{-1}) can be distinguished from S-coordination (1130−1175 cm^{-1}) and O-coordination (<1130 cm^{-1}). In ionic thiosulfates, $\nu_{as}(SO_3)$ is found at ∼1130 cm^{-1}. Thus, the strong band at 1154 cm^{-1} supports S-coordination. The symmetric SO_3 stretch near 1000 cm^{-1} (1008 cm^{-1} for this compound) is less diagnostic, but the position can be correlated to S-coordination (>1000 cm^{-1}) or O-coordination (<1000 cm^{-1})[15] and again supports the former.

(5) Brown, T. A.; Fischmann, A. J.; Spiccia, L.; McPhail, D. C. Hydrometallurgy 2003. Fifth International Conference in Honor of Professor Ian Ritchie, Vancouver, BC, Canada, Aug 24−27, 2003; 1, 213−226.
(6) Rábai, G.; Epstein, I. R. *Inorg. Chem.* **1992**, *31*, 3239−3242.
(7) Hemmes, P.; Petrucci, S. *J. Phys. Chem.* **1968**, *72*, 3986−3992.
(8) Hemmes, P.; Petrucci, S. *J. Phys. Chem.* **1970**, *74*, 467−468.
(9) Matheson, R. *J. Phys. Chem.* **1967**, *71*, 1302−1308.
(10) Podberezskaya, N. V.; Borisov, S. V.; Bakakin, V. V. *J. Struct. Chem.* **1971**, *12*, E770−E774 (English translation).
(11) Golub, G.; Lashaz, A.; Cohen, H.; Paoletti, P.; Bencini, A.; Valtancoli, B.; Meyerstein, D. *Inorg. Chim. Acta* **1997**, *255*, 111−115.
(12) Anderegg, G.; Gramlich, V. *Helv. Chim. Acta* **1994**, *77*, 685−690.
(13) Thaler, F.; Hubbard, C. D.; Heinemann, F. W.; van Eldik, R.; Schindler, S.; Fábián, I.; Dittler-Klingemann, A. M.; Hahn, F. E.; Orvig, C. *Inorg. Chem.* **1998**, *37*, 4022−4029.
(14) Nakamoto, K. *Infrared and Raman Spectra of Inorganic and Coordination Compounds*, 4th ed.; Wiley: New York, 1986.

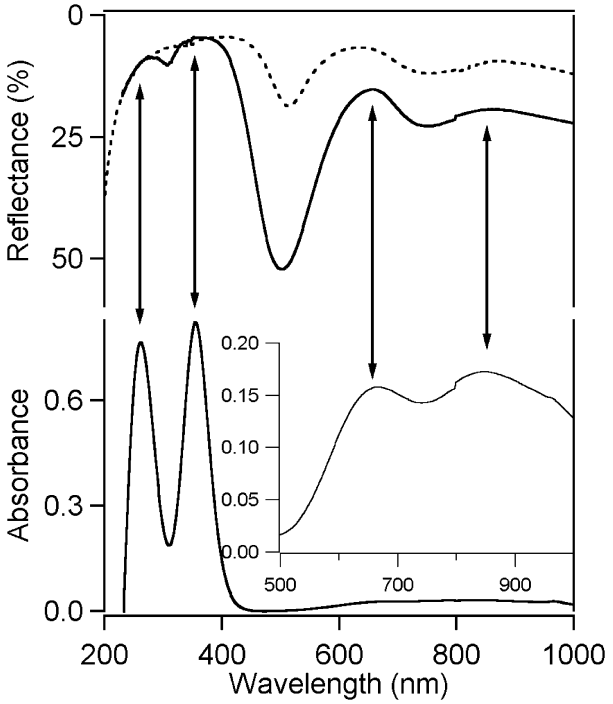

Figure 2. Comparison of the solid-state diffuse reflectance (top) and aqueous solution (bottom) electronic spectra of [Cu(tren)(S_2O_3)] (—). For solution spectrum, [Cu(tren)(H_2O)$^{2+}$] = 0.25 mM and [$S_2O_3^{2-}$] = 2.5 mM (inset: 2.5, 25 mM, respectively). The diffuse reflectance spectrum of [Cu(Bz_3tren)(S_2O_3)]·MeOH is also shown (– – –).

The IR spectrum of the green crystals of [Cu(Bz_3tren)(S_2O_3)]·MeOH indicated S-bound thiosulfate[14] [$\nu_{as}(SO_3)$ = 1157 cm^{-1}], and the ($S_2O_3^{2-}$)—Cu(II) LMCT transition in the diffuse reflectance of the UV—visible spectrum (Figure 2) matched that from the aqueous solution (367 nm). The two d—d transitions (868 and 630 nm, Figure 2) are characteristic of TBP Cu(II) geometry, as would be expected with a tripodal ligand.

Blue crystals of [Cu(Me_3tren)(MeCN)](ClO_4)$_2$ and green crystals of (H_3Me_3tren)[Cu(Me_3tren)(S_2O_3)]$_2$(ClO_4)$_3$ showed absorptions in their IR spectra confirming the presence of perchlorate, Me_3tren, MeCN (for the former), and thiosulfate (for the latter).

Crystallography. The molecular structures of the complexes reveal that the tripodal tetradentate ligands enforce a trigonal bipyramidal (TBP) Cu(II) geometry, which is typical of Cu(II) complexes of tren and derivatives thereof.[11] In each case, the bridgehead amine nitrogen occupies an axial position and the three pendant amines (either primary for tren or secondary for Me_3tren and Bz_3tren) form the equatorial plane. The remaining axial position is occupied by S-coordinated thiosulfate or acetonitrile. In the discussion to follow, the τ parameter of Addison et al.[16] is used to quantify the degree of distortion of these five-coordinate complexes from ideal trigonal bipyramidal geometry (τ = 100%) toward ideal square pyramidal geometry (τ = 0%).

[Cu(Me_3tren)(MeCN)](ClO_4)$_2$. Since the only previously published crystal structure of a Cu(II)—Me_3tren complex is that of a cyanide-bridged binuclear species, [Cu_2(Me_3tren)$_2$(CN)](ClO_4)$_3$·2MeCN,[13] the structure of [Cu(Me_3tren)(MeCN)](ClO_4)$_2$ was determined for comparison with the Cu(II)—Me_3tren—$S_2O_3^{2-}$ structure. The Cu(II) geometry of [Cu(Me_3tren)(MeCN)](ClO_4)$_2$ is almost an ideal TBP structure (τ = 94%), and acetonitrile coordinates to the free axial position via the nitrile nitrogen (Figure 3). The methyl groups point down toward the acetonitrile and radiate out symmetrically. As has been found for other Cu(II) complexes of tren-type ligands,[13] the Cu(II) center projects away from the bridgehead nitrogen, in this case, by 0.194(2) Å out of the N(2), N(3), and N(4) plane. Moderately strong H bonding between some perchlorate oxygens and the amine protons (Table 2 and Figure 4) arranges the structure into 1D chains that align at an angle to the *c* axis. One perchlorate [Cl(2)] bridges adjacent [Cu(Me_3tren)(MeCN)]$^{2+}$ cations via O(6) and O(7), whereas the other projects out from the chain and only bonds with H through O(4).

Thiosulfate Complexes. In the structure of the only compound to feature the coordination of thiosulfate to Cu(II), [Cu(en)$_2$(S_2O_3)], thiosulfate is weakly coordinated via the terminal sulfur (Cu—S bond distance of 2.71 Å) to a copper(II) center in a square pyramidal geometry.[17] The lack of crystallographic data arises because Cu(II) complexes often promote the oxidation of thiosulfate to polythionates,[6] and thiosulfate complexes are commonly too unstable to be crystallized. Crystal structures featuring the monodentate S binding of thiosulfate to other divalent transition-metal ions have been reported for Ni(II),[10,18] Co(II),[18] Zn(II),[19,20] and Pd(II)[21] (Table 4); however, none of these have TBP geometry. As observed previously,[18] the mean S—O bond distance of the Cu(II) complexes is similar to that in ionic thiosulfates (e.g., the $Na_2S_2O_3$ described below). The S—S and M—S bonds show greater variation, and for three of the complexes {[Cu(tren)(S_2O_3)]·H_2O, complex b of [Cu(Me_3tren)(S_2O_3)], and [Cu(Bz_3tren)(S_2O_3)]·MeOH}, there appears to be an inverse relationship between the S—S and M—S distances. In terms of the Pearson HSAB scheme,[22] the Pd(II) ion should favor S binding; accordingly, the Pd(II) complex has the shortest M—S and the longest S—S bond distances. When compared to those of other 3d metal ions, the M—S distances in the [Cu(L)(S_2O_3)] complexes are shorter than those of the Co(II) and Ni(II) complexes and closest to that in the Zn(II) complex.

[Cu(tren)(S_2O_3)]·H_2O (Figure 5) and [Cu(Bz_3tren)(S_2O_3)]·MeOH (Figure 6) have simple structures consisting of a

(15) Freedman, A. N.; Straughan, B. P. *Spectrochim. Acta, Part A* **1971**, *27*, 1455—1465.
(16) Addison, A. W.; Rao, T. N.; Reedijk, J.; van Rign, J.; Verschoor, G. C. *J. Chem. Soc., Dalton Trans.* **1984**, 1349—1356.
(17) Podberenzskaya, N. V.; Borisov, S. V.; Bahakin, V. V. *J. Struct. Chem.* **1971**, *12*, E770—E774 (English translation).
(18) Carter, A.; Drew, M. G. B. *Polyhedron* **1999**, *18*, 1445—1453.
(19) Baggio, R.; Baggio, S.; Pardo, M. I.; Garland, M. T. *Acta Crystallogr., Sect. C: Cryst. Struct. Commun.* **1996**, *52*, 820—823.
(20) Andreetti, G. D.; Cavalca, L.; Domiano, P.; Musatti, A. *Ric. Sci.* **1968**, *38*, 1100—1101.
(21) Baggio, S.; Amzel, L. M.; Becka, L. N. *Acta Crystallogr., Sect. B: Struct. Sci.* **1970**, *26*, 1698—1705.
(22) Pearson, R. G. In *Hard and Soft Acids and Bases*; Pearson, R. G., Ed.; Dowden, Hutchinson & Ross: Stroudsburg, PA, 1973; pp 67—107.

Table 1. Crystal Data for $[Cu(Me_3tren)(MeCN)](ClO_4)_2$ (**I**), $(H_3Me_3tren)[Cu(Me_3tren)(S_2O_3)]_2(ClO_4)_3$ (**II**), $[Cu(tren)(S_2O_3)]\cdot H_2O$ (**III**), and $[Cu(Bz_3tren)(S_2O_3)]\cdot MeOH$ (**IV**)

	I	II	III	IV
empirical formula	$C_{11}H_{27}Cl_2CuN_5O_8$	$C_{27}H_{69}Cl_3Cu_2N_{12}O_{18}S_4$	$C_6H_{20}CuN_4O_4S_2$	$C_{28}H_{40}CuN_4O_4S_2$
fw (g mol^{-1})	491.82	1211.61	339.92	624.3
T (K)	123(2)	123(2)	123(2)	123(2)
crystal system	orthorhombic	orthorhombic	monoclinic	orthorhombic
space group	*Pna*2(1)	*P*2(1)2(1)2(1)	*P*2(1)/*c*	*Pbca*
a (Å)	19.2487(3)	12.0421(3)	10.894(2)	16.1557(4)
b (Å)	8.49330(10)	12.8448(3)	10.053(2)	14.1477(4)
c (Å)	12.35080(10)	33.9332(9)	12.238(2)	26.5325(9)
β (deg)	90	90	102.36	90
V (Å^3)	2019.17(4)	5248.7(2)	1309.2(5)	6064.4(3)
Z	4	4	4	8
ρ_{calc} (g cm^{-3})	1.618	1.533	1.725	1.368
μ Mo Kα (mm^{-1})	1.394	1.196	1.996	0.897
reflections collected	27524	36419	14532	46210
independent reflections	4699	10602	3202	6941
GOF on F^2	1.05	1.088	1.045	1.024
R1,[a] wR2[b] [$I > 2\sigma(I)$]	0.0320, 0.0710	0.0940, 0.2045	0.0304, 0.0663	0.0696, 0.0951
maximum difference peak, hole (e Å^{-3})	0.744, −0.398	1.814, −0.897	0.396, −0.537	0.517, −0.478

[a] $R1 = \sum||F_o| - |F_c||/\sum|F_o|$. [b] $wR2 = [\sum w(F_o^2 - F_c^2)^2/\sum w(F_o^2)^2]^{1/2}$.

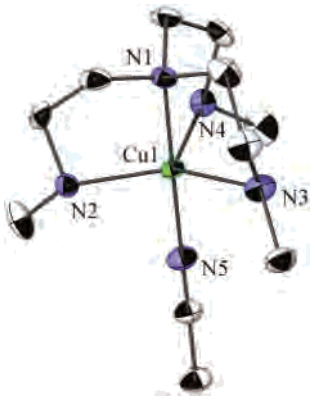

Figure 3. ORTEP view of the complex in $[Cu(Me_3tren)(MeCN)](ClO_4)_2$ (hydrogens omitted for clarity).

Table 2. Hydrogen Bonding in $[Cu(Me_3tren)(MeCN)](ClO_4)_2$ (distances in Å and angles in deg)[a]

	D−H	H···A	D···A	<(DHA)
N(2)−H(2)···O(7)[1]	0.93(4)	2.50(3)	3.263(3)	140(3)
N(4)−H(4)···O(4)[2]	0.86(4)	2.37(4)	3.199(4)	163(4)
N(3)−H(3)···O(6)	0.93(5)	2.29(5)	3.183(4)	162(4)

[a] Symmetry transformations used to generate equivalent atoms: (1) $-x + {}^1/_2, y + {}^1/_2, z + {}^1/_2$; (2) $x - {}^1/_2, -y - {}^1/_2, z$. D = donor atom; A = acceptor atom.

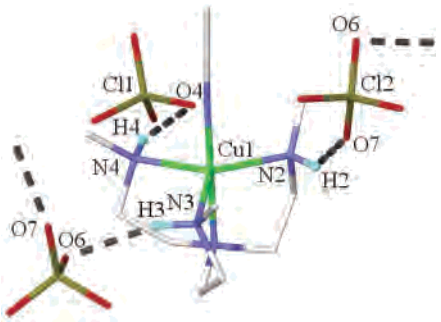

Figure 4. Hydrogen bonding in $[Cu(Me_3tren)(MeCN)](ClO_4)_2$ (non-amine hydrogens omitted).

neutral, monomeric coordination complex and a solvent molecule. The Me_3tren complex, however, contains two inequivalent $[Cu(Me_3tren)(S_2O_3)]$ moieties (Figure 7), a triply protonated Me_3tren and three perchlorate anions. One of the

Table 3. Selected Bond Distances (Å) and Bond Angles (deg) in $[Cu(Me_3tren)(MeCN)](ClO_4)_2$

Cu(1)−N(5)	1.982(3)
Cu(1)−N(1)	2.030(2)
Cu(1)−N(2)	2.080(2)
Cu(1)−N(4)	2.093(2)
Cu(1)−N(3)	2.111(3)
N(5)−C(10)	1.135(4)
C(10)−C(11)	1.449(5)
N(5)−Cu(1)−N(1)	179.3(1)
N(5)−Cu(1)−N(2)	95.1(1)
N(1)−Cu(1)−N(2)	85.3(1)
N(5)−Cu(1)−N(4)	95.6(1)
N(1)−Cu(1)−N(4)	84.72(9)
N(2)−Cu(1)−N(4)	123.2(1)
N(5)−Cu(1)−N(3)	95.2(1)
N(1)−Cu(1)−N(3)	84.0(1)
N(2)−Cu(1)−N(3)	124.1(1)
N(4)−Cu(1)−N(3)	110.2(1)
C(10)−N(5)−Cu(1)	175.2(2)
N(5)−C(10)−C(11)	178.8(3)

$[Cu(Me_3tren)(S_2O_3)]$ moieties (complex a in Figure 7) has a highly distorted geometry intermediate between TBP and square pyramidal ($\tau = 57\%$), whereas the other ($\tau = 86\%$, complex b of Figure 7) is similar to the tren and Bz_3tren complexes ($\tau = 81$ and 82%, respectively). The high degree of distortion of complex a is reflected in a tight Cu−S−S angle (<100°), which helps to accommodate the hydrogen bonding of O(2) to the $(H_3Me_3tren)^{3+}$ cation (Figure 8). The N(2)−Cu(1)−N(3) angle increases from 120 (ideal) to 139.2(4)° to permit the thiosulfate to adopt this orientation.

With the coordination to Cu(II), the S−S bond is significantly lengthened from the ionic distance[24] of 2.0054(4) Å, yet the S−O distances are indistinguishable from those in ionic compounds [1.468(4) Å].[25] As is typical for Cu(II) complexes of the tren family of ligands,[13] the axial Cu−N distance in each complex is shorter than the average equatorial distance (Table 5), and the angles between the axial nitrogen, Cu(II), and the equatorial nitrogen atoms are

(23) Freire, E.; Baggio, S.; Baggio, R.; Suescun, L. *Acta Crystallogr., Sect. C: Cryst. Struct. Commun.* **1999**, *55*, 1780−1784.
(24) Teng, S. T.; Fuess, H.; Bats, J. W. *Acta Crystallogr., Sect. C: Cryst. Struct. Commun.* **1984**, *40*, 1787−1789.
(25) Cotton, A. F.; Wilkinson, G. *Advanced Inorganic Chemistry*, 5th ed.; Wiley-Interscience: New York, 1988.

Table 4. Comparison of Geometric Parameters for Selected Thiosulfate Complexes[a]

complex	geometry	S−S bond distance (Å)	mean S−O bond distance (Å)	M−S bond distance (Å)	ref
$[Cu(tren)(S_2O_3)]\cdot H_2O$	TBP	2.051(1)	1.464	2.316(1)	this study
$[Cu(Me_3tren)(S_2O_3)]$	TBP	2.042(3), 2.014(3)	1.459	2.330(3), 2.280(3)	this study
$[Cu(Bz_3tren)(S_2O_3)]\cdot MeOH$	TBP	2.061(2)	1.460	2.301(1)	this study
$[Cu(en)_2S_2O_3]$	SP	2.05	1.47	2.71	17
$[Ni(phen)(OH_2)_3(S_2O_3)]\cdot H_2O$	O	2.003(1)	1.4731	2.449(1)	23
$[N(CH_3)_4]_2[Co(H_2O)_4(S_2O_3)_2]$	O	2.011†	1.460†	2.488†	18
$[Zn(phen)(H_2O)_2][Zn(phen)(S_2O_3)_2]\cdot H_2O$	T	2.048(3), 2.030(2)	1.449	2.252(2), 2.275(8)	19
$[Pd(en)_2][Pd(en)(S_2O_3)_2]$	P	2.061(6), 2.072(6)	1.457(7)	2.282(6), 2.312(6)	21
$Na_2S_2O_3$		2.0054(4)	1.4765	2.9638#	24

[a] Average (#); identical for both thiosulfates (†). O = octahedral; T = tetrahedral; SP = square pyramidal; P = square planar; and TBP = trigonal bipyramidal.

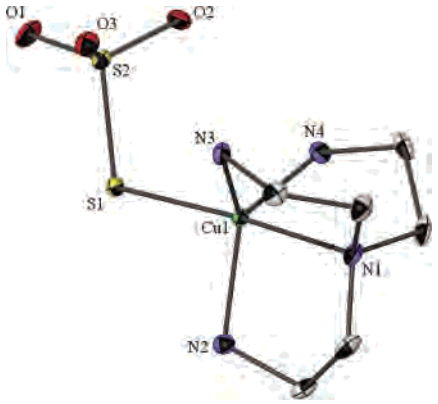

Figure 5. ORTEP view of the complex in $[Cu(tren)(S_2O_3)]\cdot H_2O$ (hydrogens omitted for clarity).

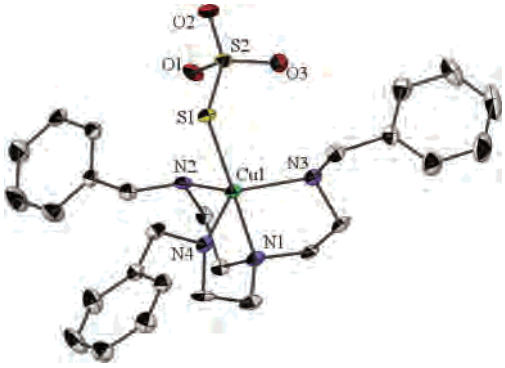

Figure 6. ORTEP view of $[Cu(Bz_3tren)(S_2O_3)]\cdot MeOH$ (hydrogens omitted for clarity).

less than 90°, which position each Cu(II) atom out of the plane defined by the equatorial nitrogen atoms toward the thiosulfate (Table 6). Compared to those of the tren complex, the axial Cu−N bonds in the Me_3tren and Bz_3tren complexes are shorter, yet the equatorial Cu−N bonds are generally longer. Such a trend is consistent with that observed by Komiyama et al.[26] (who studied the Cu(II)−chloride complexes of Bz_3tren and Me_3Bz_3tren), in which the average Cu−N_{eq} distance increased in the order tmpa < tren < Bz_3tren < Me_3Bz_3tren ≈ Me_6tren; *viz.*, the distance increased as the steric bulk of the terminal nitrogen donors increased from

(26) Komiyama, K.; Furutachi, H.; Nagatomo, S.; Hashimoto, A.; Hayashi, H.; Fujinami, S.; Suzuki, M.; Kitagawa, T. *Bull. Chem. Soc. Jpn.* **2004**, *77*, 59−72.

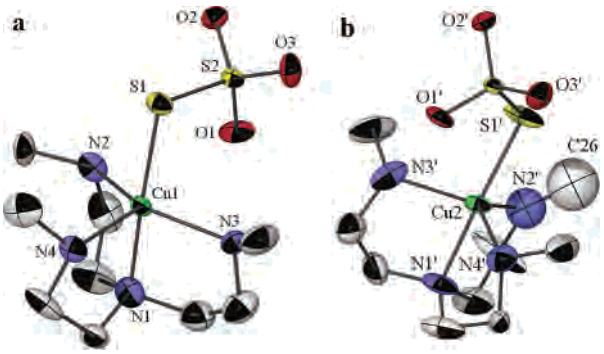

Figure 7. ORTEP view of the two inequivalent complexes (a and b) in $(H_3Me_3tren)[Cu(Me_3tren)(S_2O_3)]_2(ClO_4)_3$ (hydrogens omitted for clarity). N(2′) and C(26) in complex b were refined isotropically and are shown without the octant slice.

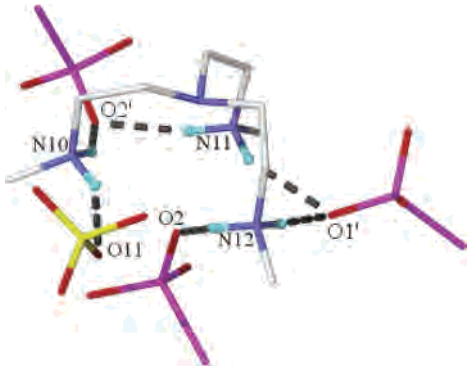

Figure 8. H-bonding interactions involving $(H_3Me_3tren)^{3+}$ (most hydrogens omitted for clarity). The major conformation (66%) of $(H_3Me_3tren)^{3+}$ is shown.

heterocyclic to primary, secondary, and tertiary amines. Me_3tren can be added to this trend as being approximately equal to Bz_3tren as a result of this work, as would be expected for a terminal donor set consisting of secondary amine nitrogens.

In each $[Cu(Me_3tren)(S_2O_3)]$ unit of $(H_3Me_3tren)[Cu(Me_3tren)(S_2O_3)]_2(ClO_4)_3$ and $[Cu(Bz_3tren)(S_2O_3)]\cdot MeOH$, the alkyl groups on the same side of the complex as the thiosulfate−SO_3 group are oriented away from the thiosulfate, whereas in $[Cu(Me_3tren)(MeCN)](ClO_4)_2$ and $[Cu(Bz_3tren)Cl]Cl$,[27] where the axial ligand is symmetrical, the alkyl groups are arranged symmetrically around the Cu(II) center (Figure 9).

Table 5. Selected Bond Lengths (Å) for Cu(II)−L−S_2O_3 Complexes

bond[a]		tren	Bz_3tren	Me_3tren (a)	Me_3tren (b)
Cu−N_{ax}	Cu−N(1)	2.075(2)	2.064(3)	2.052(9)	2.075(8)
Cu−N_{eq}	Cu−N(2)	2.047(2)	2.098(4)	2.041(8)	2.08(2)
	Cu−N(3)	2.062(2)	2.100(4)	2.103(8)	2.09(1)
	Cu−N(4)	2.112(2)	2.168(4)	2.194(7)	2.10(1)
Cu−S	Cu−S(1)	2.3158(8)	2.301(1)	2.329(3)	2.281(3)
S−S	S(2)−S(1)	2.0513(8)	2.061(2)	2.044(3)	2.014(3)
S−O	S(2)−O(1)	1.464(2)	1.465(3)	1.496(7)	1.434(7)
	S(2)−O(2)	1.461(2)	1.461(3)	1.460(6)	1.464(7)
	S(2)−O(3)	1.465(2)	1.455(3)	1.440(7)	1.458(7)

[a] N_{ax} = axial nitrogen; N_{eq} = equatorial nitrogen.

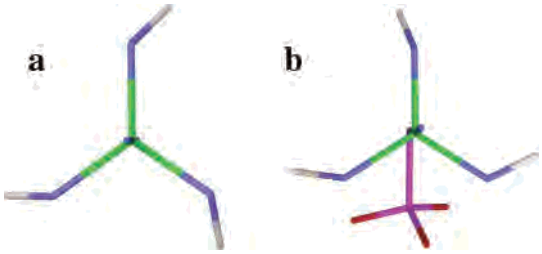

Figure 9. Orientation of methyl groups around the Cu(II) center in Me_3-tren complexes: (a) [Cu(Me_3tren)(MeCN)](ClO_4)$_2$; (b) (H_3Me_3tren)[Cu(Me_3tren)(S_2O_3)]$_2$(ClO_4)$_3$.

H-Bonding Interactions in Thiosulfate Complexes. In each complex, intramolecular H bonding exists between one or more of the N−H groups on the amine ligand and one or more of the oxygen atoms on the coordinated thiosulfate. In [Cu(tren)(S_2O_3)]·H_2O, further H bonding between adjacent [Cu(tren)(S_2O_3)] units forms two-dimensional sheets that pack along the *bc* plane and are separated from each other by H-bonded layers of water (Figure 10 and Table 7).

In [Cu(Bz_3tren)(S_2O_3)]·MeOH, the MeOH molecule bridges O(2) and H(3) through H bonding, and another H bond between H(2) and O(1) completes a 10-member ring (Figure 11a). Furthermore, [Cu(Bz_3tren)(S_2O_3)] units H bond to each other from H(3) to O(3), forming one-dimensional chains along the *b* axis. Figure 11b shows that although there is no direct interaction between the chains, they pack into pseudosheets along the *ab* plane. The hydrophobic groups (benzene rings and methyl group of the methanol) project out in the *c* direction. Figure 11c shows that the benzyl groups on adjacent pseudosheets are weakly intercalated, namely, the slight interdigitation of the aromatic ring hydrogens.

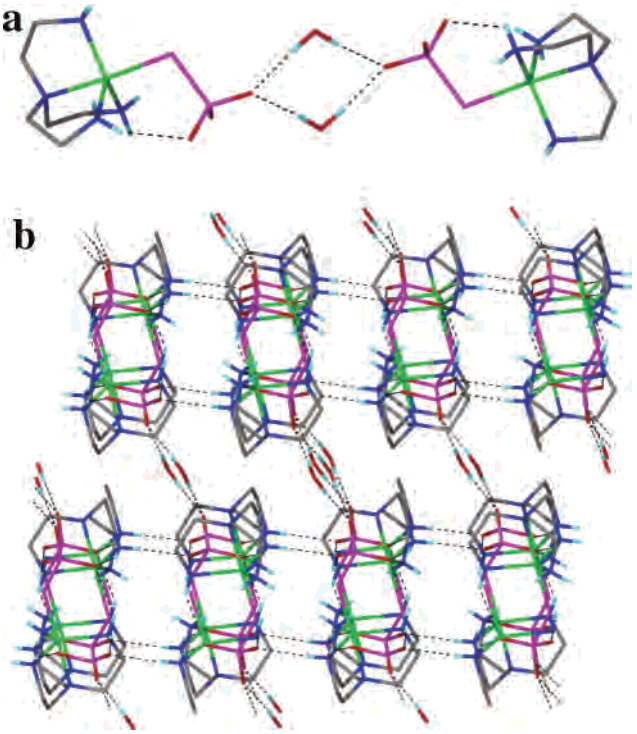

Figure 10. (a) H-bond network and (b) crystal packing showing H bonding between sheets in [Cu(tren)(S_2O_3)]·H_2O.

Similarly, (H_3Me_3tren)[Cu(Me_3tren)(S_2O_3)]$_2$(ClO_4)$_3$ exhibits intramolecular thiosulfate−amine H bonds in addition to the H-bonding interaction between $H_3Me_3tren^{3+}$ and O(2) described above. In this complex, the perchlorate anions are found to be H bonded to amine protons on adjacent complexes.

Potentiometric Titrations. The acid dissociation constants for protonated Bz_3tren, $(H_4Bz_3tren)^{4+}$, and Cu(II)−L complex formation constants were determined by potentiometric pH titrations, as described in the Experimental Section. HYPERQUAD[28] was used to analyze the data, and the results are shown in Table 8.

The substitution of benzyl groups for methyl groups dramatically lowers the pK_a values of the secondary nitrogens, and this lower affinity for protons is also reflected in the lower stability constant of the Cu(II) complex. The pK_a of the coordinated water molecule is very low compared to those of the other complexes. This is possibly due to the proximity of the hydrophobic benzyl groups which in Zn-

Table 6. Selected Bond Angles (deg) for Cu(II)−L−S_2O_3 Complexes

angle[a]		tren	Bz_3tren	Me_3tren (a)	Me_3tren (b)
N_{eq}−Cu−N_{ax}	N(1)−Cu(1)−N(4)	83.67(8)	83.9(1)	83.8(3)	81.7(4)
	N(3)−Cu(1)−N(1)	83.76(7)	83.8(1)	84.3(4)	83.1(4)
	N(2)−Cu(1)−N(1)	84.76(7)	84.1(1)	85.3(4)	84.9(5)
N_{eq}−Cu−N_{eq}	N(3)−Cu(1)−N(4)	112.97(8)	114.0(2)	106.9(3)	112.9(4)
	N(2)−Cu(1)−N(4)	117.01(8)	113.8(2)	111.1(3)	120.1(5)
	N(2)−Cu(1)−N(3)	126.85(8)	129.0(2)	139.2(4)	123.0(5)
N_{eq}−Cu−S	N(2)−Cu(1)−S(1)	91.22(6)	94.3(1)	90.6(3)	89.7(4)
	N(4)−Cu(1)−S(1)	96.85(6)	97.1(1)	102.8(2)	101.6(3)
	N(3)−Cu(1)−S(1)	99.90(6)	97.0(1)	95.3(2)	99.4(3)
N_{ax}−Cu−S	N(1)−Cu(1)−S(1)	175.71(5)	178.3(1)	173.1(3)	174.5(3)
Cu−S−S	S(2)−S(1)−Cu(1)	103.28(3)	102.52(6)	97.1(1)	109.5(1)

[a] N_{ax} = axial nitrogen; N_{eq} = equatorial nitrogen.

Table 7. Hydrogen Bonding in $[Cu(tren)(S_2O_3)]\cdot H_2O$ (**I**), $[Cu(Bz_3tren)(S_2O_3)]\cdot MeOH$ (**II**), and $(H_3Me_3tren)[Cu(Me_3tren)(S_2O_3)]_2(ClO_4)_3$ (**III**) (bond distances in Å and angles in deg)

complex	bond[a]	D−H	H···A	D···A	<(DHA)
I	N(4)−H(5)···O(3)[1]	0.83(3)	2.18(3)	2.991(3)	164(2)
	N(2)−H(6)···O(3)[2]	0.82(3)	2.17(3)	2.986(3)	173(2)
	N(4)−H(8)···O(2)	0.87(3)	2.34(3)	3.077(3)	143(2)
	N(3)−H(9)···S(1)[2]	0.80(3)	2.75(3)	3.439(2)	145(2)
	N(2)−H(14)···O(2)[1]	0.80(3)	2.17(3)	2.939(3)	159(2)
	N(3)−H(18)···S(1)[3]	0.83(2)	2.81(2)	3.564(2)	152(2)
	O(1W)−H(1W)···O(1)[4]	0.81(4)	2.18(4)	2.990(3)	176(4)
	O(1W)−H(2W)···O(1)	0.82(3)	2.08(3)	2.901(3)	174(3)
II	N(4)−H(4)···O(3)[5]	0.80(4)	2.35(4)	3.062(5)	149(4)
	N(3)−H(3)···O(5)	0.80(3)	2.41(4)	3.155(5)	155(3)
	N(2)−H(2)···O(1)	0.83(4)	2.06(4)	2.866(5)	163(3)
	O(5)−H(5)···O(2)	0.88(6)	1.94(6)	2.795(5)	162(5)
III	N(12)−H(12C)···O(2)	0.92	2.11	2.77(1)	127.1
	N(10)−H(10D)···O(11)	0.92	2.18	3.01(1)	149.1
	N(3′)−H(3′)···O(1′)	0.93	2.34	3.09(1)	137.2
	N(2)−H(2)···S(1)	0.93	2.88	3.113(8)	95.8
	N(3)−H(3)···O(1)	0.93	2.29	2.95(1)	127.9
	N(12)−H(12D)···O(1′)[6]	0.92	2.26	3.18(1)	174.6
	N(11)−H(11C)···O(1′)[6]	0.92	2.15	2.96(1)	145.8
	N(11)−H(11D)···O(2′)[7]	0.92	1.97	2.87(1)	166
	N(10)−H(10C)···O(2′)[7]	0.92	2.13	2.98(1)	154.1
	N(4′)−H(4′)···S(1)[8]	0.93	2.67	3.55(1)	157
	N(4)−H(4)···O(20)[9]	0.93	2.22	3.11(2)	160.3
	N(12)−H(12C)···O(2)	0.92	2.11	2.77(1)	127.1

[a] Symmetry transformations used to generate equivalent atoms. (1) $-x+1, y+{}^1/_2, -z+{}^3/_2$; (2) $-x+1, -y, -z+1$; (3) $-x+1, y-{}^1/_2, -z+{}^3/_2$; (4) $-x, -y, -z+1$; (5) $-x+{}^1/_2, y-{}^1/_2, z$; (6) $x+1, y, z$; (7) $x+{}^1/_2, -y-{}^1/_2, -z$; (8) $x-1, y, z$; (9) $-x+1, y-{}^1/_2, -z+{}^1/_2$. D = donor atom; A = acceptor atom.

(II) complexes and enzymes is responsible for increasing the acidity of coordinated water.[29]

Thiosulfate Binding Constants. The striking spectral changes in the 300−450 nm region were used to determine the thiosulfate binding constant to $[Cu(L)(H_2O)]^{2+}$ (Figure 12). This was preferred to the minor changes in the visible spectrum due to the d−d bands.

Matrix decomposition was applied to the absorbance data to determine the spectrum and concentration of each absorbing complex. The EQBRM program[30] was used through the Matlab interface to calculate speciation from a chemical model consisting of mass-balance (including charge balance) and mass-action equations for Na^+, ClO_4^-, $NaClO_4$, MOPS, $MOPS^-$, NaMOPS, $S_2O_3^{2-}$, $[Cu(L)(H_2O)]^{2+}$, and $[Cu(L)(S_2O_3)]$, where appropriate. The procedure has been recently described in detail by Brugger et al.[31] Examples of the fit to the data are given for $[Cu(tren)(H_2O)]^{2+}$ and $[Cu(tren)(S_2O_3)]$ (Figure 12), and the calculated molar absorbance spectrum of each thiosulfate complex is shown in Figure 13. The calculated position of the S−Cu(II) LMCT maximum was in agreement with the diffuse reflectance of the UV−visible spectrum of the corresponding solid compound {note that no comparison is possible for $[Cu(Me_6tren)(S_2O_3)]$, for which no solid product could be obtained}.

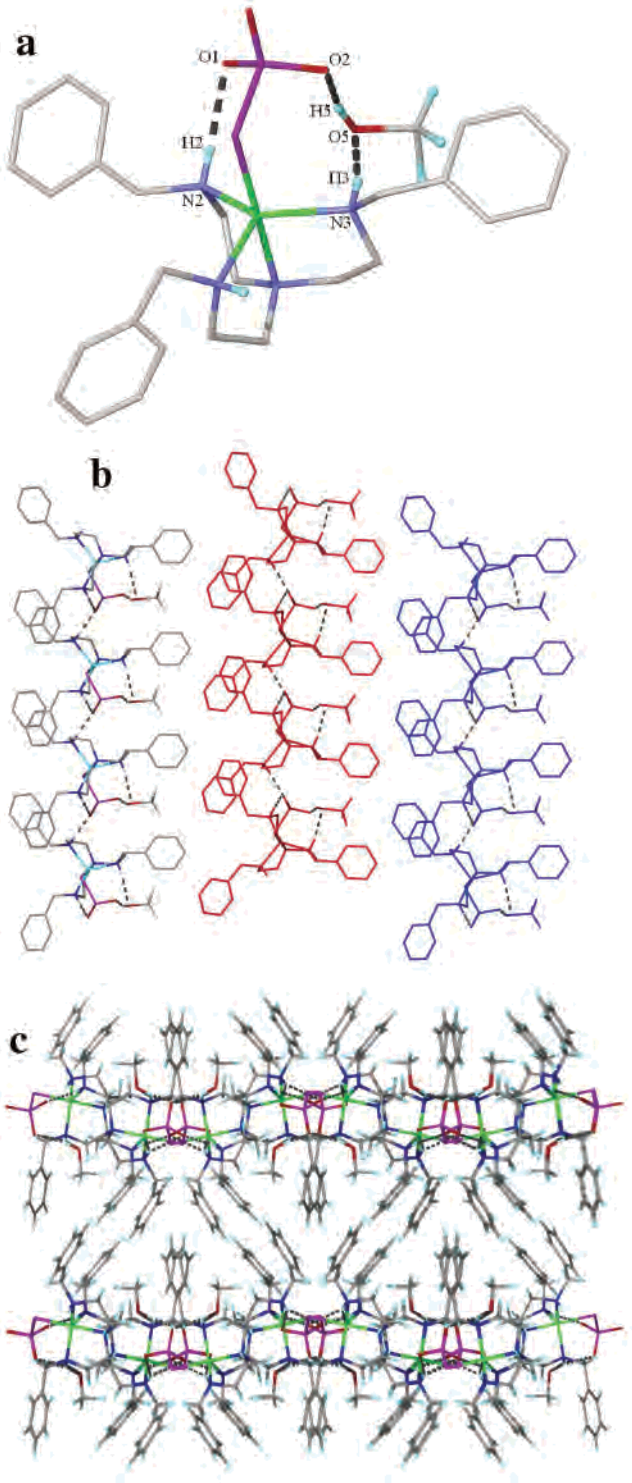

Figure 11. (a) Moderately strong H bonding forming the 10-member ring (most hydrogens omitted for clarity), (b) packing of chains along the *ab* plane into a pseudosheet (most hydrogens omitted for clarity), and (c) weak intercalation of aromatic rings between pseudosheets in $[Cu(Bz_3tren)(S_2O_3)]\cdot MeOH$.

The formation constants for $[Cu(tren)(S_2O_3)]$ [$K_f = (1.82 \pm 0.09) \times 10^3\ M^{-1}$], $[Cu(Me_3tren)(S_2O_3)]$ [$(2.13 \pm 0.05) \times 10^3\ M^{-1}$], and $[Cu(Bz_3tren)(S_2O_3)]$ [$(4.30 \pm 0.21) \times 10^4\ M^{-1}$] are higher than those for any other divalent transition-

(27) Schatz, M.; Becker, M.; Walter, O.; Liehr, G.; Schindler, S. *Inorg. Chim. Acta* **2001**, *324*, 173−179.
(28) Gans, P.; Sabatini, A.; Vacca, A. *Talanta* **1996**, *43*, 1739−1753.
(29) Mareque-Rivas, J. C.; Prabaharan, R.; Parsons, S. *J. Chem. Soc., Dalton Trans.* **2004**, 1648−1655.
(30) Anderson, G. M.; Crerar, D. A. *Thermodynamics in Geochemistry: The Equilibrium Model*; Oxford University Press: New York, 1993.
(31) Brugger, J.; McPhail, D. C.; Black, J.; Spiccia, L. *Geochim. Cosmochim. Acta* **2001**, *65*, 2691−2708.

Table 8. pK_a Values of tren-Based Ligands and Formation Constants for $[CuL(H_2O)]^{2+}$ and $[CuLH(H_2O)]^{3+}$ and pK_a Values for the Ligated Water in $[CuL(H_2O)]^{2+}$ [25.0 ± 0.1 °C, I = 1 M ($NaClO_4$)][a]

ligand	pK_{a1}	pK_{a2}	pK_{a3}	pK_{a4}	log K_{CuL}	log K_{CuLH}	p$K_{a(CuL)}$	ref
tren	10.42(1)	9.88(1)	8.915(5)	<1	19.58(3)	13.22(4)	9.4	12
Me_3tren	10.93(1)	10.24(1)	9.17(1)	<1	19.11(2)		9.08(2)	13
Bz_3tren[b]	9.16(1)	8.56(2)	7.17(3)	1.2(1)	15.10(4)	3.77(7)	7.10(9)	this study
Me_6tren	10.13(1)	9.32(1)	8.17(1)	<1	15.65(3)	9.53(4)	8.1	12

[a] Numbers in parentheses are the standard deviations in the last digit. [b] I = 0.1 M ($NaNO_3$); $K_{CuL} = [CuL^{2+}]/([Cu^{2+}][L])$; $K_{CuLH} = [Cu(LH)^{3+}]/([Cu^{2+}][LH^+])$.

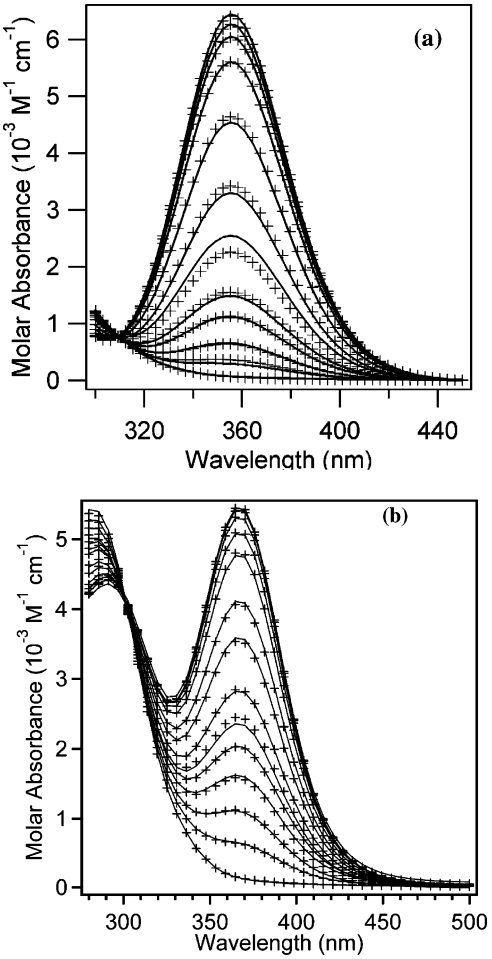

Figure 12. Changes in UV spectrum with thiosulfate concentration: measured data (−) and fit (+) for (a) $[Cu(tren)(H_2O)]^{2+}$ and (b) $[Cu(Bz_3tren)(H_2O)]^{2+}$.

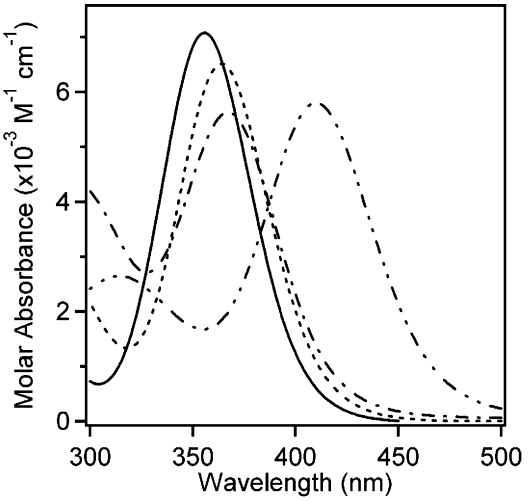

Figure 13. Calculated spectra of $[Cu(L)(S_2O_3)]$ complexes; L = tren (—) λ_{max} 356 nm, Me_3tren (− −) λ_{max} 364 nm, Bz_3tren (− · −) λ_{max} 367 nm, and Me_6tren (− ·· −) λ_{max} 410 nm.

metal ion (Table 9) and, in particular, higher than that for $[Cu(en)_2(S_2O_3)]$ (the most closely related complex shown). The only other reported Cu(II)−thiosulfate formation constant is the β_2 value for $[Cu(S_2O_3)_2]^{2-}$, which cannot be compared directly with K_f for $[Cu(L)(S_2O_3)]$. The thiosulfate binding constants for other divalent transition-metal ions (Ni^{2+}, Zn^{2+}, Co^{2+}, and Mn^{2+}) are 1−2 orders of magnitude smaller than those for the above Cu(II) complexes.

There is no clear correlation between the measured stability constants and crystallographic measurements of bonding strength (i.e., S−S and Cu−S distances) and the location of the Cu(II) center relative to the tripodal plane. Crystal packing effects may be masking any relationship that may be present.

$[Cu(Me_6tren)(S_2O_3)]$ differs from the other three complexes in that its formation constant is much lower (40 ± 10 M^{-1}), and that it oxidizes thiosulfate in the presence of an excess of thiosulfate. Golub et al.[11] concluded from their study of anions binding to $[Cu(tren)(H_2O)]^{2+}$ and $[Cu(Me_6tren)(H_2O)]^{2+}$ that N-methylation of tren caused the copper(II) center to behave as a stronger and harder Lewis acid. The thiosulfate binding constants are in agreement, and the harder Cu(II) ion in $[Cu(Me_6tren)(H_2O)]^{2+}$ has the weakest binding interaction with the soft thiosulfate-S. However, the Bz_3tren binding constant seems anomalous because $[Cu(Bz_3tren)(H_2O)]^{2+}$ is more acidic than $[Cu(Me_6tren)(H_2O)]^{2+}$ (7.1 vs 8.3), but in this case, the aromatic groups may be influencing the acidity of the coordinated water, as seen in the Zn(II) complexes mentioned above,[29] and the interaction of thiosulfate with the copper(II) center.

The mechanism of the electron-transfer process that gives rise to oxidation of thiosulfate and concurrent reduction of Cu(II) is unclear as there are literature examples of both inner-sphere and outer-sphere reactions. The fact that the LMCT for the Me_6tren complex is at lower energy indicates that electron transfer within this system is more facile, while the lower binding constant means that the concentrations of free $[Cu(Me_6tren)(H_2O)]^{2+}$ and $S_2O_3^{2-}$ in solution would be higher for this system than for the others; therefore, the rate of an outer-sphere electron-transfer process involving the reaction between $[Cu(Me_6tren)(H_2O)]^{2+}$ and either the $[Cu(Me_6tren)(S_2O_3)]$ complex or free $S_2O_3^{2-}$ would be enhanced. A detailed kinetic investigation of this reaction is in progress to attempt to elucidate the mechanism of these complex reactions.

The Me_3tren and the Bz_3tren complexes not only exhibit the highest thiosulfate binding constants of the four com-

Table 9. Comparison of Constants for the Binding of Thiosulfate to Divalent Metal Ions at 25 °C

reaction	method[a]	ionic strength	log K_f	ref
$[Cu(Bz_3tren)(H_2O)]^{2+} + S_2O_3^{2-} \leftrightarrows [Cu(Bz_3tren)(S_2O_3)] + H_2O$	spec	0.03−0.04 M	4.63	this study
$[Cu(Me_3tren)(H_2O)]^{2+} + S_2O_3^{2-} \leftrightarrows [Cu(Me_3tren)(S_2O_3)] + H_2O$	spec	0.15 M	3.31	this study
$[Cu(tren)(H_2O)]^{2+} + S_2O_3^{2-} \leftrightarrows [Cu(tren)(S_2O_3)] + H_2O$	spec	0.25 M	3.26	this study
$[Cu(Me_6tren)(H_2O)]^{2+} + S_2O_3^{2-} \leftrightarrows [Cu(Me_6tren)(S_2O_3)] + H_2O$	spec	0.15 M	1.60	this study
$Cu^{2+} + 2S_2O_3^{2-} \leftrightarrows [Cu(S_2O_3)_2]^{2-}$	spec	0.2 M	4.56[b]	6
$[Cu(en)_2(H_2O)_2]^{2+} + S_2O_3^{2-} \leftrightarrows [Cu(en)_2(S_2O_3)] + 2H_2O$	spec	0.0 M[c]	2.28, 2.34	7, 8
	spec	0.0 M[c]	2.2−2.5	9
$Ni^{2+} + S_2O_3^{2-} \leftrightarrows [Ni(S_2O_3)]$	cal	0.50 M	0.78	32
$Zn^{2+} + S_2O_3^{2-} \leftrightarrows [Zn(S_2O_3)]$	cal	0.5 M	1.12	32
	ext	1.00 M	0.62	33
	pot	2.0 M	1.10	34
	pot	3.0 M	0.96	35
$Co^{2+} + S_2O_3^{2-} \leftrightarrows [Co(S_2O_3)]$	cal	0.50 M	0.77	32
$Mn^{2+} + S_2O_3^{2-} \leftrightarrows [Mn(S_2O_3)]$	cal	0.5 M	0.67	32

[a] Spec = spectrophotometric, cal = calorimetric, ext = solvent extraction, and pot = potentiometric. [b] Value is $\log_{10} \beta_2$, not $\log_{10} K_f$. [c] Results of experiments at different ionic strengths extrapolated to $I = 0$.

plexes measured but also are the least reactive in terms of thiosulfate oxidation. This observation suggests that the oxidation reaction may not be proceeding via an intramolecular electron-transfer process; otherwise, an increase in reactivity would be expected. Moreover, the intermolecular or outer-sphere pathway is blocked because the strong binding of thiosulfate leaves very little free $[Cu(L)(H_2O)]^{2+}$ in solution to react with either free thiosulfate or the thiosulfate complex. Due to the low solubility of $[Cu(Bz_3tren)(H_2O)]^{2+}$, whether thiosulfate oxidation is possible when an excess of the Cu(II) complex is present, this theory cannot be tested as it has been for tren.[5]

Conclusions

The results presented herein demonstrate that relatively minor modifications of tris(2-aminoethyl)amine, achieved through N-alkylation, result in copper(II) complexes with significantly different thiosulfate binding characteristics and abilities to promote the oxidation of thiosulfate. The much higher reactivity, lower stability, and lower-energy LMCT transition of $[Cu(Me_6tren)(S_2O_3)]$, when compared with those of the other three complexes, have yet to be fully rationalized. The origin of this behavior will be further explored through studies of the copper(II) complexes of other tren derivatives with all tertiary amine donors. This work demonstrates that large differences in reactivity between Cu(II) and thiosulfate can be brought about through functionalization of amine ligands. Such a result may be promising for gold processing applications; if a Cu(II)−L complex is found that is satisfactory in terms of gold oxidation properties and the thiosulfate oxidation behavior inhibited through the choice of spectator ligand, then the potential exists for developing improved gold leaching agents.

Experimental Section

Materials and Reagents. Me_6tren,[36,37] Bz_3tren,[38] $[Cu(tren)(H_2O)](ClO_4)_2$,[39] and $[Cu(Me_6tren)(H_2O)](ClO_4)_2$[40] were synthesized by published procedures with minor modifications. The synthesis of $[Cu(Me_3tren)(H_2O)](ClO_4)_2$ was based on the method used for $[Cu(Me_6tren)(H_2O)](ClO_4)_2$. All other chemicals were used as received from commercial suppliers and were of analytical grade unless otherwise indicated. Water was freshly distilled prior to use, and CO_2-free water was prepared by boiling distilled water under nitrogen for 2 h.

Instrumentation. UV−vis−NIR spectra were recorded on a Varian Cary 5G spectrophotometer fitted with a water-jacketed cell holder. An externally circulating water bath (Varian) maintained the temperature to a precision of ±0.1 °C. Quartz cells (1 cm) were first rinsed with distilled water and then with the sample prior to use.

Solution pH was measured on either a Metrohm electrode, fitted to a Metrohm pH meter, or a Eutech electrode, fitted to an EcoScan pH 5−6 meter. A Metrohm 736 GP Titrino was used to dispense the small volumes of NaOH solution required to fix the pH of the samples for $[Cu(tren)(S_2O_3)]$. All pH measurements were made at 25 °C (temperature maintained by a Haake W 19 water bath). The electrodes were calibrated using standard phthalate, phosphate, and borate buffer solutions.

IR spectra were recorded on a Perkin-Elmer 1600 spectrometer as KBr disks or Nujol mulls. Elemental analyses were performed by Campbell Microanalytical Service, Otago University, Otago, New Zealand. ^{1}H NMR spectra were recorded in $CDCl_3$ on either a Bruker AC200 or Bruker DPX300 spectrometer. The residual solvent peak was used as an internal standard. Mass spectra were recorded on a Biomass Platform II mass spectrometer using an electrospray ionization source.

Me_6tren. Yield: 20%. ^{1}H NMR δ (ppm): 2.23 [$-N(CH_3)_2$, s, 18H], 2.35, 2.38, 2.40, 2.42, 2.59, 2.61, 2.63, 2.66 ($-CH_2CH_2-$, m, 12H). ESI-MS *m*/*z* (ion, %): MH^+ 231.1 (100), MNa^+ 253.2 (15), MK^+ 269.1 (8).

Bz_3tren. Yield: 66%. ^{1}H NMR δ (ppm): 1.64 (NH, br s), 2.55−2.71 (m, 12H, CH_2CH_2), 3.74 (6H, CH_2Ph), 7.21−7.33 (m, C_6H_5),

(32) Aruga, R. *J. Inorg. Nucl. Chem.* **1974**, *36*, 3779−3782.
(33) Moriya, H.; Sekine, T. *Bull. Chem. Soc. Jpn.* **1974**, *47*, 747−748.
(34) Nazarova, L.; Efremova, T.; Orenshtein, S. *Russ. J. Inorg. Chem.* **1972**, *17*, 186−188.
(35) Persson, H. *Acta Chem. Scand.* **1970**, *24*, 3739−3750.
(36) Giumanini, A. G.; Chiavari, G.; Scarponi, F. L. *Anal. Chem.* **1976**, *48*, 484−489.
(37) Ciampolini, M.; Nardi, N. *Inorg. Chem.* **1966**, *5*, 41−44.
(38) Naiini, A. A.; Menge, W. M. P. B.; Verkade, J. G. *Inorg. Chem.* **1991**, *30*, 5009−5012.
(39) Fry, F. Polynuclear Metal Complexes of Macrocyclic Ligands and their Ability to Hydrolyse Phosphate Esters. Ph.D. Thesis, Monash University, Melbourne, AU, 2002.
(40) Lee, S. C.; Holm, R. H. *J. Am. Chem. Soc.* **1993**, *115*, 11789−11798.

7.11−7.36 (m). ESI-MS *m*/*z* (ion, %): 417 MH^+ (>98%); minor peak at 327 indicates $Bz_2tren\ H^+$ (<2%).

[Cu(tren)(S_2O_3)]·H_2O. Copper perchlorate hexahydrate (0.579 g, 1.56 mmol) and tris(2-aminoethyl)amine (0.240 g, 1.64 mmol) were dissolved in a minimum of distilled water and formed a deep-blue solution. Upon addition of sodium thiosulfate pentahydrate (0.386 g, 1.56 mmol), the solution became dark green. Some solid remained in the bottom of the vial. A sample of the supernatant solution (∼1.5 mL) was taken and left to evaporate in air over a period of 3 weeks. The blue and white solid residue was then dissolved in a minimum of distilled water, and EtOH was added to give a green solution. This was sealed and placed in the freezer. After 10 days, small blue and green crystals had formed. One blue and one green crystal were analyzed by single-crystal XRD, and both were found to be [Cu(tren)(S_2O_3)]·H_2O.

A second batch of the complex was made by dissolving [Cu(tren)(H_2O)](ClO_4)$_2$ (0.306 g, 0.7 mmol) in a minimum of distilled water and by adding $Na_2S_2O_3$·$5H_2O$ (0.175 g, 0.7 mmol), dissolved in a minimum volume of distilled water. EtOH was added until precipitation of a fine green solid occurred, and the suspension was placed in the freezer. Flaky green crystals formed overnight. These were washed with Et_2O (80 mL) and dried in a desiccator. Yield = 0.162 g (67%). At this point, the product was analyzed by IR spectroscopy (results are the same as for the sample obtained above). The flaky green crystals were redissolved in a minimum quantity of distilled water and placed in an evaporating dish. Diamond-shaped dark-green crystals, with the same unit-cell dimensions as those above, formed overnight on evaporation of the water. Characterization microanalyses. Found (%): C, 21.4; H, 5.9; N, 16.4. Calcd for $C_6H_{20}N_4O_4S_2Cu$ (%): C, 21.2; H, 5.9; N, 16.5. Selected IR bands [KBr, ν (cm^{-1})]: 3548 (s), 3478 (s), 3269 (s), 3159 (s), 2880 (s), 1612 (m), 1473 (m), 1154 (s), 1066 (m), 1008 (s), 902 (m), 638 (s), 459 (m). Diffuse reflectance UV−vis−NIR spectrum [λ_{max}, nm (reflectance, %)]: 280 (8.5), 360 (4.5), 655 (15), 860 (19.5). Solution UV−vis−NIR spectrum (H_2O) [λ_{max}, nm (molar absorbance, $M^{-1}\ cm^{-1}$)]: 257 (2930), 356 (4910), 686 (110), 853 (130). ESI-MS *m*/*z* (ion, %) $H_2O\backslash CH_3OH$: 209 (100), 211 (43) [Cu(tren)]$^+$; 344 (94), 346 (51) [Cu(tren)(S_2O_3)]·Na^+; 322 (4), 344 (3) [Cu(tren)(S_2O_3)]·H^+.

[Cu(Bz_3tren)(S_2O_3)]·MeOH. Bz_3tren (0.205 g, 0.5 mmol) was dissolved in 10 mL of a 1:1 H_2O/MeOH mixture. To this solution were added $Cu(ClO_4)_2$·$6H_2O$ (0.185 g, 0.5 mmol) and $Na_2S_2O_3$·$5H_2O$ (1.239 g, 5 mmol). Immediately when the thiosulfate was added, a dark-green solid formed and was separated by vacuum filtration. The dark-green filtrate was left to stand (covered) for 2 days, whereupon fine dark-green needles (unsuitable for crystallography) and plates (used in X-ray structure determination) formed. Characterization (needles and plates) microanalyses. Found (%): C, 51.7; H, 5.9; N, 8.8. Calcd for $C_{27}H_{40}CuN_4O_5S_2$ (i.e., replacement of MeOH with 2 × H_2O): C, 51.7; H, 6.4; N, 8.9. Selected IR bands [KBr, ν (cm^{-1})]: 3423 (br), 3230 (m), 2926 (w), 2897 (w), 1619 (m), 1457 (m), 1157 (s), 1000 (s), 743 (m), 703 (m), 640 (s). Diffuse reflectance UV−vis−NIR spectrum [λ_{max}, nm (reflectance, %)]: 868 (9), 630 (7), 403 (5), 302 (7). Solution UV−vis−NIR spectrum (MeCN) [λ_{max}, nm (molar absorbance, $M^{-1}\ cm^{-1}$)]: 268 (4860), 275 (4900), 287 (4930), 391 (5480), 637 (330), 871 (330).

[Cu(Me_6tren)(H_2O)](ClO_4)$_2$. Synthesis followed a published method[40] with minor modifications to the workup. Typically, to a hot solution of $Cu(ClO_4)_2$·$6H_2O$ (2.785 g, 7.5 mmol) in 30 mL of EtOH (pale-blue solution) was added a solution of Me_6tren (1.743 g, 7.6 mmol) in 18 mL of EtOH, resulting in a dark-blue solution, which gave the product on workup. Yield: 1.117 g (29%). Characterization microanalyses. Found (%): C, 28.2; H, 6.5; N, 10.8. Calcd for $C_{12}H_{32}Cl_2CuN_4O_9$ (%): C, 28.3; H, 6.3; N, 11.0. Selected IR bands [KBr, ν (cm^{-1})]: 3449 (br), 2981 (m), 2898 (m), 2850 (m), 1474 (s), 1148 (s), 1094 (s), 1005 (m), 624 (s). Diffuse reflectance UV−vis−NIR spectrum [λ_{max}, nm (reflectance, %)]: 871 (8), 700 sh (16), 330 (5), 280 sh (7). Solution UV−vis−NIR spectrum (H_2O) [λ_{max}, nm (molar absorbance, $M^{-1}\ cm^{-1}$)]: 290 (4270), 710 sh (160), 875 (450).

[Cu(Me_3tren)(H_2O)](ClO_4)$_2$. Synthesis was based on the method published for [Cu(Me_6tren)(H_2O)](ClO_4)$_2$.[40] Typically, Me_3tren (Aldrich; 0.943 g, 5 mmol) was reacted with a hot solution of $Cu(ClO_4)_2$·$6H_2O$ (1.857 g, 5 mmol) in 20 mL of EtOH. Yield: 1.526 g (65%). Characterization microanalyses. Found (%): C, 23.5; H, 5.7; N, 12.1. Calcd for $C_9H_{26}Cl_2CuN_4O_9$ (%): C, 23.1; H, 5.6; N, 12.0. Selected IR bands [KBr, ν (cm^{-1})]: 3500 (br), 3273 (m), 2882 (m), 1473 (m), 1091 (s), 626 (s). Diffuse reflectance UV−vis−NIR spectrum [λ_{max}, nm (reflectance, %)]: 871 (9), 669 (9), 320 (5), 263 (8). Solution UV−vis−NIR spectrum (MeCN) [λ_{max}, nm (molar absorbance, $M^{-1}\ cm^{-1}$)]: 274 (3770), 690 sh (100), 854 (230).

[Cu(Me_3tren)(MeCN)](ClO_4)$_2$. Slow diffusion of Et_2O into 6 mL of a MeCN solution of [Cu(Me_3tren)(H_2O)](ClO_4)$_2$ (0.05 g, 0.1 mmol) yielded dark-blue crystals after 3 weeks. Yield: 0.019 g (38%). Characterization. Selected IR bands [Nujol, ν (cm^{-1})]: 3259 (s), 2723 (m), 2319 (s), 2291 (s), 2022 (s), 1715 (w), 1660 (w), 1294 (s), 1220 (s), 1086 (br), 621 (s). Diffuse reflectance UV−vis−NIR spectrum [λ_{max}, nm (reflectance, %)]: 323 (10), 664 (14), 847 (15). Solution UV−vis−NIR spectrum (MeCN) [λ_{max}, nm (molar absorbance, $M^{-1}\ cm^{-1}$)]: 284 (7480), 646 sh (90), 820 (270).

(H_3Me_3tren)[Cu(Me_3tren)(S_2O_3)]$_2$(ClO_4)$_3$. [Cu(Me_3tren)(H_2O)](ClO_4)$_2$ (0.091 g, 0.2 mmol) was dissolved in 6 mL of MeOH to give a bright-blue solution. $Na_2S_2O_3$·$5H_2O$ (0.049 g, 0.2 mmol) was added to [Cu(Me_3tren)(H_2O)](ClO_4)$_2$ (0.091 g, 0.2 mmol) in 6 mL of MeOH (bright blue), and the color changed to dark green. Not all of the thiosulfate dissolved. Dark-green crystals formed upon diffusion of Et_2O into this solution. Yield: 0.049 g (40%). Microanalyses. Found (%): C, 26.8; H, 5.9; N, 13.8. Calcd for $C_{27}H_{75}Cl_3Cu_2N_{12}O_{18}S_4$ (%): C, 26.6; H, 6.2; N, 13.8. Selected IR bands [KBr, ν (cm^{-1})]: 3449 (br), 3263 (s), 2926 (m), 2888 (m), 1477 (m), 1457 (m), 1192 (s), 1146 (sh), 1087 (s), 990 (s), 859 (m), 830 (m), 649 (s), 623 (s). Diffuse reflectance UV−vis−NIR spectrum [λ_{max}, nm (reflectance, %)]: 290 (5), 379 (4), 684 (17), 894 (11). Solution UV−vis−NIR spectrum (MeCN) [λ_{max}, nm (molar absorbance, $M^{-1}\ cm^{-1}$)]: 282 (8600), 383 (6190), 686 sh (465), 850 (724).

X-ray Crystallography. Single-crystal X-ray data were collected on an Enraf-Nonius CAD4 diffractometer with monochromated Mo Kα radiation (λ = 0.71073 Å) at 123(2) K using φ and/or ω scans. Data were corrected for Lorentz and polarization effects, and absorption corrections were applied. The structure was solved by the direct methods and refined using the full-matrix least-squares method of the programs SHELXS-97[41] and SHELXL-97,[42] respectively. The program X-Seed[43] was used as an interface to the SHELX programs and to prepare the figures. Most hydrogen atoms were located on Fourier difference maps and refined isotropically; otherwise, they were modeled in idealized geometries. All of the non-hydrogen atoms were refined anisotropically, except O(22), O(30)−(33), N(2′), and C(26) in [Cu(Me_3tren)(S_2O_3)]$_2H_3Me_3$tren(ClO_4)$_3$, which were modeled isotropically. C(30) and C(31), C(34)

(41) Sheldrick, G. M. *SHELXS-97*; University of Göttingen: Göttingen, Germany, 1997.
(42) Sheldrick, G. M. *SHELXL-97*; University of Göttingen: Göttingen, Germany, 1997.
(43) Barbour, L. J. *J. Supramol. Chem.* **1999**, *1*, 189−191.

Table 10. Concentrations Used for Potentiometric Titrations

volume ratio (Cu/L)	0	1:2	1:1.3	1:1
$[Cu(II)]_{total}$ (mM)	0.0	1.7	2.1	2.5
$[Bz_3tren]_{total}$ (mM)	5.0	3.3	2.9	2.5

and C(35), and C(38) and C(39) were refined as being disordered across two positions in a 2:1 ratio, respectively.

Potentiometric Titrations. Solutions for pH tirations were prepared using CO_2-free water, and each titration was performed in duplicate in a sealed vessel under a nitrogen atmosphere. $NaNO_3$ and $Cu(NO_3)_2 \cdot 2.5H_2O$ were used due to the low solubility of $[Cu(Bz_3tren)(H_2O)](ClO_4)_2$ in the presence of the slightest excess of ClO_4^-. The volume of the Bz_3tren solution (5 mM) was constant (20 mL) for each titration, whereas the volume of the Cu(II) solution (5 mM) was varied (0, 10, 15, and 20 mL). NaOH solutions (~0.1 M) were standardized against dried potassium hydrogen phthalate. The number of moles of H^+, Cu^{2+}, and Bz_3tren were refined in the fit and did not differ significantly from the calculated values based on the quantity of reagents used.

Spectrophotometric Studies. For the tren system, the pH was fixed but not buffered. For all of the other systems, MOPS (3-morpholinopropanesulfonic acid) was used. Solutions were left to equilibrate for at least 10 min in the water-jacketed cell holder ($T = 25.0 \pm 0.1$ °C) prior to measurement.

[Cu(tren)(S_2O_3)]. $Na_2S_2O_3 \cdot 5H_2O$ and $[Cu(tren)(H_2O)](ClO_4)_2$ were used to volumetrically prepare stock solutions of thiosulfate (75 mM) and the Cu(II) complex (0.75 mM), whereas perchlorate solutions were prepared by neutralization of a standardized NaOH solution (~2 M) with perchloric acid. The thiosulfate solution was kept in the dark, and if it was not used within 2 weeks, a fresh solution was prepared. Solutions for UV−visible spectrophotometric study were prepared by mixing 10 mL each of a $[Cu(tren)(H_2O)](ClO_4)_2$ solution, a sodium thiosulfate solution, and a sodium perchlorate solution in a sealable glass vial ($[S_2O_3^{2-}]_{final} = 0.125-25.0$ mM, $I = 0.25$ M). The pH of each sample was then fixed by the addition of a small volume of NaOH from the autoburet such that the volume change upon the addition of base was less than 2%.

[Cu(Me_3tren)(S_2O_3)]. $[Cu(Me_3tren)(H_2O)](ClO_4)_2$, MOPS, and $NaClO_4 \cdot H_2O$ were used to volumetrically prepare a Cu stock solution in deoxygenated water, which had a composition of $[Cu]_{total} = 0.5$ mM, $[MOPS]_{total} = 100$ mM and $I = 0.15$ M. The pH of the stock was adjusted to 7.50 at 25 °C by titration with an approximately 1 M NaOH solution and then stored in a refrigerator. Thiosulfate stock solutions (50, 20, and 0.5 mM; $I = 0.15$ M) were prepared with deoxygenated water using $Na_2S_2O_3 \cdot 5H_2O$ and $NaClO_4 \cdot H_2O$ and used to prepare a series of solutions with concentrations in the 0.5−50 mM range, which were stored in a refrigerator until required. Samples for spectrophotometric measurement were prepared by mixing 2 mL of each thiosulfate solution with 2 mL of the Cu(II) complex stock solution. The UV−visible spectrum of each sample was measured from 200 to 500 nm with the appropriate background solution in the reference beam. The spectra of the Cu(II)-free background solutions were measured and subtracted from the measured spectra.

[Cu(Me_6tren)(S_2O_3)]. Both copper(II) and thiosulfate stock solutions were prepared in the same way as for [Cu(Me_3tren)(S_2O_3)]. The final concentrations of the solutions used in spectral analysis were $[Cu]_{total} = 0.25$ mM, $[S_2O_3^{2-}] = 0-25$ mM, and $I = 0.15$ M ($NaClO_4$). Due to the reactivity of $[Cu(Me_6tren)(H_2O)]^{2+}$ with thiosulfate, a two-compartment mixing cell was used to allow the two solutions to equilibrate to 25 ± 0.1 °C in the cell prior to mixing. The UV−visible spectrum was then recorded from 300 to 500 nm within approximately 1 min of mixing, and the baseline spectra were subtracted as above prior to analysis.

[Cu(Bz_3tren)(S_2O_3)]. In this case, the Cu(II) complex was prepared in situ. Bz_3tren and MOPS were added to deoxygenated water, the pH was adjusted to 7.50 using ~1 M NaOH, and $Cu(ClO_4)_2 \cdot 6H_2O$ was added to generate a solution with $[Cu]_{total} = 1$ mM, $[Bz_3tren]_{total} = 1$ mM, and MOPS (50 mM). It was not possible to fix the ionic strength using $NaClO_4 \cdot H_2O$ because even the slightest addition caused precipitation of a pale-blue solid, presumably of $[Cu(Bz_3tren)(H_2O)](ClO_4)_2$. Solutions for spectral measurement were prepared by mixing the Cu(II) solution with various thiosulfate solutions such that the final concentrations were $[Cu]_{tot} = 0.5$ mM, $[S_2O_3^{2-}] = 0-2.5$ mM, and $I = 0.03-0.04$ M. Spectral measurements were conducted as they were for [Cu(Me_3tren)(S_2O_3)].

Acknowledgment. We are grateful to the ARC Center for Green Chemistry, the Australian Postgraduate Award Scheme (A.J.F. and J.B.), and the Australian Institute for Nuclear Science and Engineering for financial support, to Ms. A. Kutasi for kindly collecting the X-ray data for the Bz_3tren and Me_3tren complexes, and to Dr. S. R. Batten for assistance with modeling the disorder in the crystal structure of $(H_3Me_3tren)[Cu(Me_3tren)(S_2O_3)]_2(ClO_4)_3$.

Supporting Information Available: Crystallographic data for $[Cu(Me_3tren)(MeCN)](ClO_4)_2$, $[Cu(tren)(S_2O_3)] \cdot H_2O$, $[Cu(Bz_3tren)(S_2O_3)] \cdot MeOH$, and $(H_3Me_3tren)[Cu(Me_3tren)(S_2O_3)]_2(ClO_4)_3$ in CIF format. This material is available free of charge via the Internet at http://pubs.acs.org.

IC0492800